Shh signaling is essential for rugae morphogenesis in mice.

Dae-Woon Kang

The Graduate School

Yonsei University

Department of Dentistry

Shh signaling is essential for rugae morphogenesis in mice.

Directed by Professor Byung-Jai Choi

The Doctoral Dissertation
Submitted to the Department of Dentistry
and the Graduate School of Yonsei University
in partial fulfillment of the requirements for
the degree of
Doctor of Philosophy

Dae-Woon Kang

December 2010

This certifies that the Doctoral Dissertation of
Dae-Woon Kang is approved

_____
Byung-Jai Choi

_____
Jae-Ho Lee

_____
Hyung-Jun Choi

_____
Syng-Ill Lee

_____
Han-Sung Jung

The Graduate School
Yonsei University
December 2010

ACKNOWLEDGEMENTS

먼저 대학원 진학에 큰 힘이 되어 주시고 끝없는 관심과 애정으로 오늘이 있게 해주신 최병재 교수님께 감사드립니다. 또한 이 논문이 완성되기까지 끊임없는 관심과 배려 그리고 세심한 지도를 베풀어 주신 정한성 교수님께도 진심으로 감사드립니다.

논문의 작성과 심사에 많은 지도편달을 해 주신 이제호, 최형준, 이승일교수님의 격려에 깊은 감사를 드립니다. 그리고 처음부터 끝까지 바쁜 와중에도 많은 도움을 준 구강생물학교실의 조성원교수와 이종민 선생님께도 큰 감사를 드립니다.

치과의사로서 경영자로서 발전할 수 있도록 자극을 주는 고운미소치과 동료들에게도 감사를 드립니다.

끝으로 제가 이 자리에 있기까지 아낌없이 베푸셨던 아버지, 어머니, 장인어른, 장모님 그리고 무엇보다도 항상 옆에서 힘이 되어 주는 아내 조정미와 아들 창현 그리고 박사과정중 태어난 막내 지민이에게 무한한 사랑을 전하며 이 논문을 바칩니다.

2010년 12월

저자 씀

<TABLE OF CONTENTS>

<LIST OF FIGURES>

ABSTRACT

Shh signaling is essential for rugae morphogenesis in mice.

Dae-Woon Kang

Department of Dentistry
The Graduate School, Yonsei University
(Directed by Professor Byung-Jai Choi)

Secondary palate development in mammals is a critical process that depends on complex cellular and molecular events. Corrugated structures of palatal ridges, or rugae palatinae, are observed on the hard palate region in most mammalian species, but their number and arrangement are species specific. Nine palatal ridges are found on the mouse secondary palate. Reciprocal signaling of epithelial–mesenchymal interactions plays a pivotal role in the growth of the secondary palate. Epithelial *Shh* (sonic hedgehog) signaling is closely related to both the mesenchymal *Fgf* (fibroblast growth factor) and *Bmp* (bone morphogenetic protein) pathways. Mice possess secreted Hh (hedgehog) ligands that bind to the membrane-bound receptors *Ptch1* and *Ptch2*. *Gli1* and *Glil2* are transcriptional activators of Hh signaling. *Wnt* family members including LEF1 (lymphoid enhancer factor 1) may play a functional role in orofacial morphogenesis. Maternal transfer of 5E1 (an anti-Shh antibody) to mouse embryos through the placenta, and mathematical analysis were used to demonstrate that *Sostdc1*, a secreted inhibitor of the *Wnt* pathway, is a downstream target of *Shh*. We suggest that

interactions between *Wnt*, *Shh*, and *Sostdc1* underlie a pivotal mechanism controlling the spatial patterning of palatal ridges.

Key words: rugae patterning, 5E1, *Shh* ,*Wnt*, *Sostdc1*

Shh signaling is essential for rugae morphogenesis in mice.

Dae-Woon Kang

Department of Dentistry
The Graduate School, Yonsei University
(Directed by Professor Byung-Jai Choi)

I. Introduction

1. Rugae development

The development of mammalian secondary palate is a critical mechanism dependent upon complex cellular and molecular events (Gritli-Linde, 2007). Two palatal shelves grow bilaterally to each other and then fuse at the midline to separate the nasal cavity from the oral cavities (Ferguson, 1978). Cleft palate, one of the most common birth defects in human is induced by failure of this process (Gritli-Linde, 2007). Secondary palate can be divided into the ossified hard palate and the posterior muscular soft palate. Corrugated structures of palatal ridges or rugae palatinae, are observed on the hard palate region of most mammalian species, but their number and arrangement are species specific (Eisentraut, 1979; Pantalacci *et al*., 2008).

At least nine palatal rugae are found on the mouse secondary palate. A tenth ruga (ruga 7b, Fig.1) is more or less frequently present, depending on the strain (Charles *et al.,* 2007; Peterkova R,1987). Just behind the incisor teeth, three transverse ridges are formed that span the midline of secondary palate.A further six rugae are observed around the molar tooth areas,

which have an oblique arrangement and, unlike the three transverse ridges, do not span the midline (Sakamoto *et al*., 1989; Pantalacci *et al*., 2008) (fig.1). Many nerve fibers that respond to touch and pressure on the palate are located in the palatal ridges (Mitsui *et al*., 2000; Ichikawa *et al*., 2001; Kido *et al*., 2003; Nunzi *et al*., 2004).

Local thickening of the palatal epithelium which forms placodes and the condensation of underlying mesenchymal cells are the first step of rugae development. (Fig2) and then placodes bulge toward oral cavity and incline caudally. This subsequent bulging forms a corrugated rugae appearance.

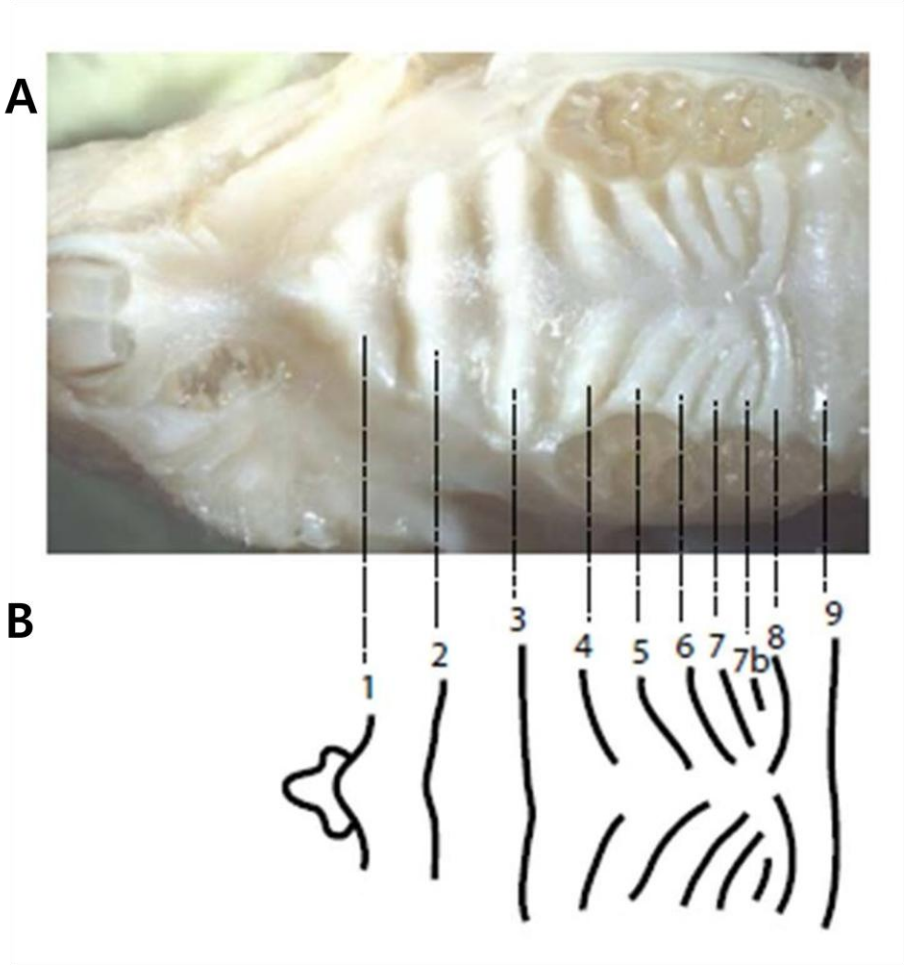

Fig.1. Adult mouse rugae pattern (A) The roof of the oral cavity of an adult mouse showing the palatal ridges (*rugae palatinae*) on the hard palate (Pantalacci *et al*., 2008). (B) Mouse rugae pattern with numbering . Note that ruga 7b was called 8b in other studies (Peterkova *et al*., 1987; Charles *et al*., 2007)

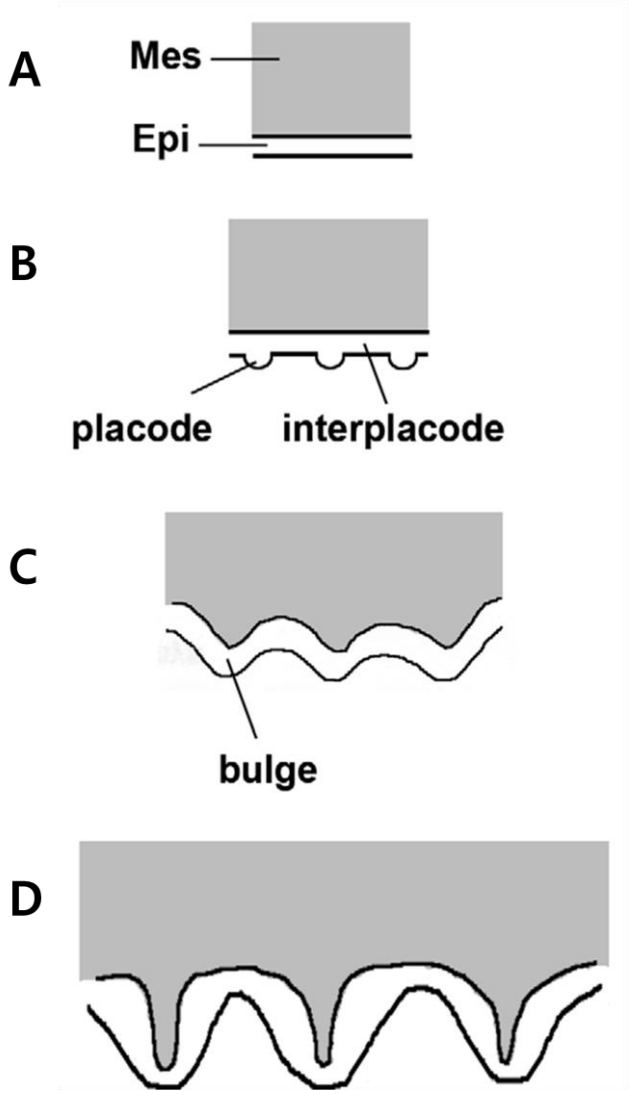

Fig.2. Developmental stages of palatal rugae (sagittal view). (A) Mes, mesenchyme; Epi, epithelium (Porntaveetus *et al*., 2010). (B) Local thickening of the palatal epithelium to form placodes. (C) Thickened epithelium protrudes on the surface of developing palate. (D) The placode regions bulge towards oral cavity to form an overall corrugated appearance (Porntaveetus *et al*.,2010).

2. Signaling events in mouse rugae development

Cell signaling plays an important role in the development of all multicellular organisms. Reciprocal growth factor signaling between the palatal mesenchyme and epithelium is important for the early growth and patterning of palatal shelves (Gorlin *et al*., 2001; Gritli-Linde, 2007; Rice *et al*., 2004; Tyler and Koch, 1977). Numerous studies have established the importance of Hedgehog signaling in a wide variety of regulatory function during the development. Previous study reported that epithelial *Shh*(sonic hedgehog) signaling is closely related to both mesenchymal *Fgf*(fibroblast growth factor) and *Bmp*(bone morphogenetic protein) pathway. These signaling molecules are involved in a cascade that regulates cellular events such as proliferation during palatogenesis (Rice *et al*., 2004; Zhang *et al*., 2002). *Shh* exhibits a restricted expression pattern in the thickened palatal ridge epithelium regions, forming the transverse rugae on the secondary palate (Bitgood and McMahon, 1995). It has also been shown that *Shh* signaling plays essential roles in craniofacial development with targeted null mutation in *Shh* resulted in various cranial defects in mice (Chiang *et al*., 1996). Mice possess secreted Hh(Hedgehog) ligands that bind to the membrane-bound receptors *Ptch1* or *Ptch2*. The *Ptch1* receptor is a target of Hh signaling and provides a negative feedback mechanism to regulate it. *Gli1* and *Gli2* are transcriptional activators of Hh signaling (Chen and Struhl, 1996; Goodrich *et al*., 1996, 1997).

Wnt family members may play a functional role in orofacial morphogenesis (Brown *et al*., 2003; Blanton *et al*., 2004; Juriloff *et al*., 2006; Lan *et al*., 2006; Lee *et al*., 2008). Lymphoid enhancer factor 1(LEF1) is expressed in most embryonic tissues, including neural crest, somites, primitive streak, and palate, and plays an important role for epithelial-mesenchymal transition(EMT) (Mohamed *et al*., 2004; Nawshad and Hay, 2003). Ohazama *et al*. (2008) reported that *Sostdc1*(also known as USAG-1, Ectodin and Wise) inhibits the *Wnt* pathway. *Lrp4* is a negative *Wnt* co-receptor antagonizing the LRP(low-density lipoprotein receptor-

related protein) 5/6-mediated activation of the *Wnt* signaling pathway (Johnson *et al*., 2005).

In this study, to reveal the mechanism of palatal rugae pattern formation, we injected 5E1(an IgG1 monoclonal antibody against Shh protein) through the placenta in order to block *Shh* signaling (Wang *et al*., 2000), and investigate the subsequent morphological changes in the rugae. In addition , the genetic relationship between *Shh* and other genes was examined to further elucidate the mechanism regulating the specific patterning of palatal ridges. Our findings show that crosstalk between *Wnt*, *Shh* and *Sostdc1* governs palatal ridge patterning during mouse palatogenesis.

II. Materials and methods

All experiments were performed according to the guidelines of the Yonsei University, College of Dentistry, Intramural Animal Use and Care Committee.

1. Experimental animals

Adult Institute of Cancer Research (ICR) mice were housed in a temperature-controlled room (22℃) under artificial illumination (lights on from 0500 to 1700 hours) and 55% relative humidity. The mice had access to food and water ad libitum. Embryos were obtained from time-mated pregnant mice. E0 was designated as the day a vaginal plug was confirmed. Embryos at developmental stages E12.5, E13.5, E14.5, E16.5 and post natal (PN) 2wks were used in this study.

2. Drug delivery

A monoclonal antibody (mAb) to 5E1 (an IgG1 monoclonal antibody against Shh protein) was obtained from hybridoma cells at the Developmental Studies Hybridoma Bank, developed under the auspices of the National Institute of Child Health and Human Development and maintained by the University of Iowa, Department of Biological Sciences (Iowa City, IA, USA). A single injection of 5E1 (10 mg/kg body weight) or PBS (1 ml) was administered intraperitoneally to pregnant ICR mice at the stage of embryonic day E12.5.

3. Scanning electron microscopy (SEM) visualization

The surface topography of the hard palate and rugae was studied by scanning electron microscopy in 3 groups composed of E12.5 wild type embryo, E16.5 embryo 4 days after maternal injection of 5E1 and E16.5 embryo 4 days after maternal injection of PBS injection as a control.

The palate, which were removed from the maxilla, were prefixed with 2.5% glutaraldehyde in PBS for 24hours at 4℃, rinsed with PBS for 8hours at 4 ℃, and postfixed with 1% osmium tetroxide in PBS for 2 hours. The sample were then dehydrated in a graded series of ethanol, followed by critical point drying using a HCP-2 apparatus (HITACHI, TOKYO, JAPAN) with CO_2 as the transitional fluid. The specimen, which were mounted on stubs, were coated with platinum and examined by scanning electron microscopy (SEM, S-3000; HITACHI, TOKYO, JAPAN).

4. Whole mount *in situ* hybridization

4.1 Embryo processing

Samples which sacrificed at 1day after 5E1 and PBS (phosphate-buffered saline) injection were fixed 24 hours in 4% paraformaldehyde in PBS hand dechorionated and dehydrated overnight in methanol at -20℃.

4.2 Riboprobe synthesis

The plasmid was linealised, to allow transcription, using an appropriate restriction endonuclease. 50 μg of DNA was digested in a final volume of 100 μl of the appropriate 10 X buffer, 2~3 μl of restriction endonuclease and rest RNase free water. This was incubated at 37℃ for 2 hours before running aliquot on a 1% agarose gel to check the DNA was completely linealised. The linealised DNA was cleaned by Qiagen Clean up Kit (Qiagen, USA)

Riboprobes were made in batches of 20 μl as follows:

4 μl 5 X buffer, 4 μl 0.1 M DTT, x μl linealised DNA (to give approximately 5 μg DNA present), 1.5 μl Dig RNA , 2 μl Polymerase, 2 μl RNase inhibitor were prepared and RNase free water was added to a final volume of 20 μl. The mixture was incubated at 37℃ for 2 hours before running aliquot on a 1% agarose gel to check the presence of an RNA band. Then, treat with 4 μl DNaseI RNase free and incubated at 37℃ for 30 mins.

RNA purification

15 µl 3M sodium acetate and add 125 µl 100% cold EtOH. Incubate at -20 ℃ for 30 mins. Centrifuge at 4 ℃, 1200 rpm for 10 mins. Discard the flowing through. Wash with 500 µl 70% cold EtOH. Discard the flowing through. Centrifuge at 4 ℃, 1200 rpm for 10 mins. Drying up all of EtOH at room temperature. Redissolve in 40 µl RNase free water. Store at 70 ℃. Before use Riboprobe, incubate at 85 ℃ for 4 mins and 2 mins in ice

4.3. Pre-hybridization treatment and hybridization

Then the samples were rehydrated stepwise in methanol/PBS and finally put back in 100% PBT (PBS with 0.1% Tween 20). Embryos older than the beginning of somitogenesis were treated with proteinase K (10 mg/ml in PBT). Samples were postfixed in 4% paraformaldehyde in PBS for 20 minutes and then rinsed in PBT 5 times for 5 mins each. The embryos were prehybridized at least 1 hour at 70℃ in hybridization buffer [50% formamide, 5 X SSC, 50 mg/ml heparin, 500 mg/ml tRNA, 0.1% Tween 20]. The hybridization was done in the same buffer containing 200 ng of probe overnight at 70℃.

4.4 Post-hybridization treatment

Then the samples were washed at 70℃ for 2 times 15 mins in 2 X SSC, 2 times 30 mins in 10% CHAPS, 2 X SSC, 2 times 15 minutes in 10% CHAPS, 1 X SSC, 2 times 15 mins in 10% CHAPS, 0.2 X SSC, 2 times 15 mins in 10% CHAPS, 0.1 X SSC. Further washes were performed at room temperature for 2 times 5 mins in TBT (1 M Tris (pH7.5), 5M NaCl, DEPC-H_2O), and then 3 hours in TBT with 2 mg/ml FBS (Fetal Bovine Serum (Clontech, USA)). Then the samples were incubated overnight at 4℃ with the preabsorbed alkaline phosphatase-coupled anti-digoxigenin antiserum (described in Boehringer instruction manual) at a 1/5000 dilution in TBT buffer containing 2 mg/ml FBS. Finally the samples were washed 2 times for 15 minutes each in TBT at room temperature. Detection was performed in alkaline phosphatase reaction buffer described in

the Boehringer instruction manual. When the color was developed, the reaction was stopped in 1 X PBS.

4.5 Solutions and buffers for whole mount *in situ* hybridization

All solutions were autoclaved where appropriate.

PBT

PBS, 0.1% (v/v) Tween-20 (Sigma, USA)

Prehybridization solution (for 50 ml)

25 ml deionized formamide (50% final), 12.5 ml 20X SSC, pH 4.5 (25% final), 50 µl 10 mg/ml Heparin stock (50 µg/ml final) (Sigma, USA), 50 µl 50 mg/ml Yeast-tRNA (50 µg/ml final) (Sigma, USA), 250 µl 1 M EDTA (5 mM final; ethylenediamine tetra acetic acid), 200 µl Tween-20 (0.4% final), 1 g Boheringer Blocking Powder (2% final), 0.5 ml CHAPS (0.1% final, 10% stock in RNase free water) (Sigma, USA) were prepared, and RNase free water was added to a final volume of 50 ml

20X SSC

3 M NaCl, 0.3 M sodium citrate, pH 4.5 with citric acid

Blocking solution

15% heat-inactivated lam serum in PBT

TBT (for 1 L)

50 ml 1 M Tris-Cl (pH 7.5), 33.33 ml 5 M NaCl, 10 ml Tween-20, RNase free water was added to a final volume of 1 L

NTMT (for 50 ml)

5 ml 1 M Tris-Cl (pH 9.5), 1 ml 5 M NaCl, 2.5 ml 1 M MgCl2, 0.5 ml Tween-20, 41 ml

water

5. Microarray analysis

Gene-chip expression analysis was performed with RNA from palatal shelves from embryos of pregnant mice at one day after injection (PBS, n=2; 5E1, n=2), using a mouse gene microarray (GeneChip Mouse Genome 430 2.0, Affymetrix, Santa Clara, CA, USA). A gene-chip scanner (GeneChip Scanner 3000, Affymetrix) was used to measure the intensity of the fluorescence emitted by the labelled target. . Raw image data were converted to cell-in tensity (CEL) files using the Affymetrix Gene Chip Operating System, and these resultant CEL files were normalized using the MARS 5.0 algorithm. Following statistical analysis, differ entially expressed genes were selected using GenePlex software version 3.0 (ISTECH, Korea). Differentially expressed genes with changes of 1.5- to 2.0-fold in the 5E1-treated group compa red with the control group were selected, and then analysed statistically using Student′s *t*-test with the level of statistical significance set at $P<0.01$

6. Real-time quantitative polymerase chain reaction(RT-qPCR)

Total RNA was isolated from the E13.5 mouse palate with 5E1 or PBS maternal injection using an RNeasy® Mini kit (Qiagen). For cDNA synthesis, reverse transcription was performed using M-MuLV reverse transcriptase (New England BioLabs). RT-qPCR was performed using the Thermal Cycler Dice™ Real Time System (TP800, Takara) with SYBR Premix EX Taq™ (Takara). The amplification program consisted of 45 cycles of denaturation at 95℃ for 5 s, annealing at 55℃ for 20 s, and extension at 72℃ for 20 s. The results of RT-qPCR for each sample were normalized to beta-2-microglobulin (β2m). The data were analyzed with Thermal Cycler Dice™ Real Time System analysis software (Takara) and expressed as normalized ratios. Data were expressed as the mean ± S.D.

7. Immunohistochemistry and TUNEL assay

E 13.5, E14.5 Embryos were fixed with 4% (w/v) paraformaldehyde (PFA) in 0.01 M phosphate-buffered saline (PBS, pH 7.4), sectioned at 7 μm, and stained with Hematoxylin-Eosin (H&E). For immunohistochemistry, sections were blocked in 0.3% hydrogen peroxide for 15 mins. The tissue sections were boiled in 10 mM citrate buffer (pH 6.0) for 20 mins and cooled at room temperature for 20 mins. The slides were incubated with primary antibody at 4℃ overnight. Slides were incubated in antibody against Ki67 (Thermo Scientific, USA). After washing with PBS, the specimens were sequentially incubated with secondary antibody and streptavidin peroxidase at room temperature for 10 mins each. Finally, staining was visualized using a diaminobenzidine reagent kit (Invitrogen, USA), and sections were counterstained with hematoxylin. A TUNEL assay was performed using an in situ cell apoptosis detection kit (Trevigen) following the manufacturer's instructions. The 7-μm-thick sections were treated with proteinase K [in 10 mM Tris–HCl (pH 8.0)] at a concentration of 20 μg/ml for 15–20 mins at room temperature. The samples were then incubated with the labeling reaction mixture at 37 ℃ for 1 h and streptavidin–HRP solution for 10 mins at room temperature. DAB was used as a substrate solution to detect the sites of in situ apoptosis under a light microscope. At least 10 specimens were examined in each experiment.

8. Protein-bead implantation

Affi-Gel blue beads (Bio-Rad Laboratories, Hercules, CA, USA) were soaked with the Shh recombinant protein (1 μg/μl; mouse Shh-N, R&D systems, Minneapolis, MN, USA). Control beads were prepared similarly by soaking them in PBS at room temperature for at least 1 hours. The palatal shelves of E12 mice were dissected and incubated in Dispase II (Roche, Mannheim, Germany) at 1.2 U/ml in PBS for 50 mins on ice, and the palatal

epithelium and mesenchyme were separated. Beads were placed on palatal mesenchyme, which was then cultured for 1 day in DMEM/F12. Whole-mount *in-situ* hybridization was then carried out.

9. Computer simulation

In order to construct a model of pattern formation for palatal rugae in wild-type mice, a system of reaction–diffusion equations was examined. The equations used are

$$\partial A/\partial t = (C_1 A - C_2 I + C_3) - C_a A + D_a \nabla^2 A$$

$$\partial M/\partial t = (C_4 A - C_5 M + C_6) - C_m A + D_m \nabla^2 M$$

$$\partial I/\partial t = (- C_7 A + C_8 M) - C_i A + D_i \nabla^2 I$$

(D : diagonal matrix of diffusion coefficients)

where A, M and I are activator, mediator and inhibitor concentrations respectively. The lower and upper limits for the synthesis rates of A ($C_1 A - C_2 I + C_3$), M ($C_4 A - C_5 M + C_6$) and I ($- C_7 A + C_8 M + C_9$) are set as

$$0 \leq (C_1 A - C_2 I + C_3) \leq synA_{max}$$

$$0 \leq (C_4 A - C_5 M + C_6) \leq synM_{max}$$

$$0 \leq (- C_7 A + C_8 M) \leq synI_{max}$$

where $synA_{max}$ = 0.4, $synM_{max}$ = 0.7 and $synI_{max}$ = 0.6. Other parameters are D_a = 0.04, D_m = 0.5, D_i = 0.1, C_1 = 0.12, C_2 = 0.04, C_3 = 0.08, C_4 = 0.47, C_5 = 0.2, C_6 = 0.06, C_7 = 0.37, C_8 = 0.32, C_a = 0.1, C_m = 0.1 and C_i = 0.1. Simulations were carried out on two-dimensional grids. The initial and final field size was 36 × 72 and 72 × 180 respectively. In order to simulate the anterior-posterior extension of the palate, a new row of cells was inserted into the anterior part of the #8 ruga for each 400 iteration after 10,000 iterations. The concentrations of each factor in new cells were set to the mean of the values in

adjacent cells. The lateral extension was simulated by adding a new column of cells to the edge of the field for each 700 iteration after 30,000 iterations. Neumann boundary condition was used for calculation. The time step was set as $dt = 0.01$. Calculation was performed with 70,000 iterations.

III. Results

1. Dotted shape of rugae patterning are observed after 5E1 treatment.

In order to confirm the relationship between rugae development and *Shh*, we injected 5E1, an antibody against Shh, to the abdomen of pregnant mice at embryonic day(E) 12.5 ; phosphate-buffered saline (PBS) was injected into control mice instead of 5E1. The mice were sacrificed 96 hours later. At the injection stage, E12.5, the palatal shelves were distant from each other and two or three rugae could be observed on their surface (green box in Fig. 3A and D). At 96 hours after PBS injection(control condition), the secondary palate was fused. Moreover, nine rugae could be clearly detected in the secondary palate region (Fig. 3B). The shape of rugae resembled a mountain range (Fig. 3E). At 96 hours after 5E1 injection, the palatal shelves had also fused, as in the controls (Fig. 3C); however, the nine ridges observed in the secondary palate of the controls could not be seen in the 5E1 injected mice. The rugae displayed a loss of their mountain-range shape, and had a dotted appearance (Fig. 3F). This dotted ridge shape was maintained up to 2weeks posnatally (Fig. 3G, H).

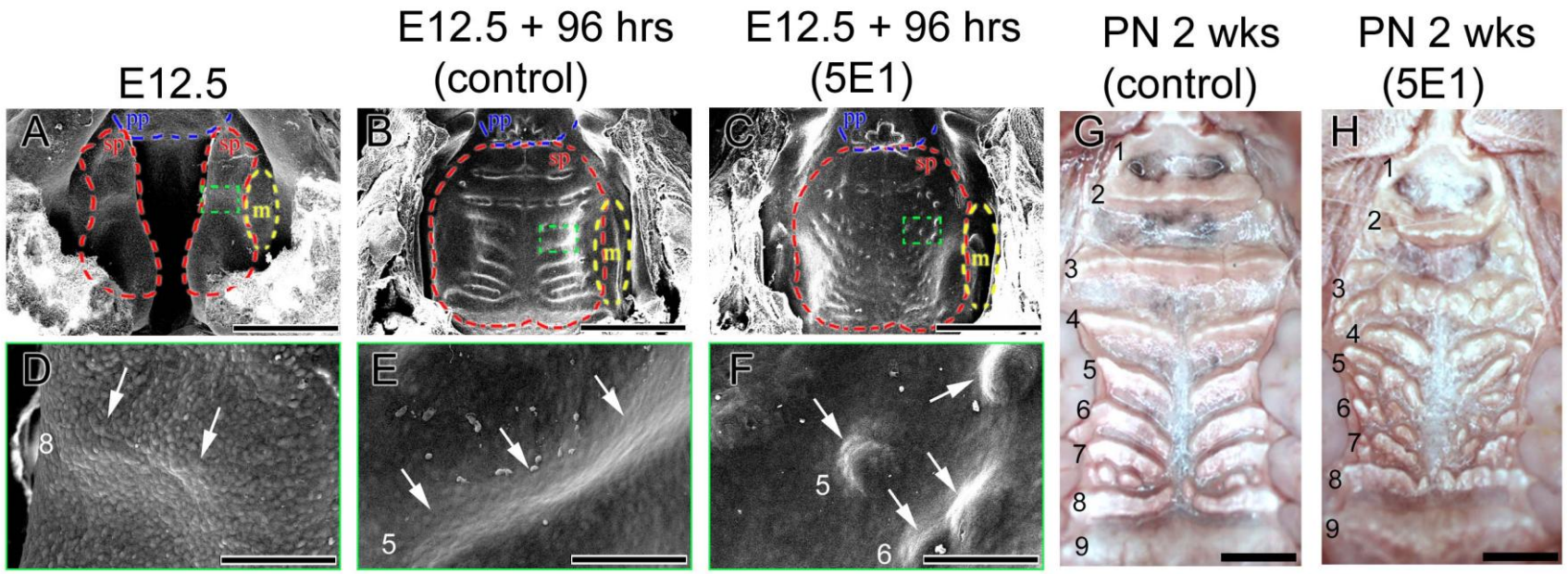
E12.5
E12.5 + 96 hrs (control)
E12.5 + 96 hrs (5E1)
PN 2 wks (control)
PN 2 wks (5E1)
A
B
C
D
E
F
G
H
PP
sp
m
8
5
6
1
2
3
4
5
6
7
8
9

Fig.3. Morphological changes in palatal rugae spatial patterning after 5E1 injection. (A, D) At E12.5, palatal shelves are not fused. Two palatal ridges are observed in each palatal shelf. (B, E) At E16.5, nine palatal ridges are detected in fused secondary palate. (C, F) After 5E1 injection, rugae patterning is changed. Nine rugae lines are not observed and dotted rugae shape is detected in fused secondary palate. (G) Stripe shape of nine palatal ridges are observed in PN 2 wks PBS treated group. (H) Dotted shape rugae are detected in PN 2 wks 5E1 injected group. Note that rugae numbering is followed in other study (Pantalacci *et al.*, 2008).Blue dotted line; primary palate, Red dotted line; secondary palate, Yellow dotted line; molar, scale bar; A-C : 1 mm, D-F : 100 μm.

2. *Wnt-, Shh-* and *Sostdc1-* related gene expression patterns are disrupted when *Shh* activity is blocked by 5E1 injection.

The relationship between rugae formation and gene expression was investigated by performing *in situ* hybridization 24 hours after 5E1 injection. After PBS injection, *Shh* was expressed strongly along the rugae line, with its expression pattern mimicking the adult mountain-range-like rugae shape (Fig. 4A). Examination of sagittal sections showed that *Shh* was strongly expressed at the epithelial tip of palatine rugae (Fig. 4A`). However, the *Shh* expression pattern was changed after 5E1 injection. 5E1 induced expansion of the region of *Shh* expression in developing rugae (Fig. 4E). After sectioning, the region of *Shh* expression was much wider than in the PBS-treated controls (Fig. 4E`). *Sostdc1* was strongly expressed in the epithelium of the developing palate, except along the rugae lines (Fig. 4B and B`). After 5E1 injection, *Sostdc1* expression was clearly reduced during palatogenesis compared to the PBS-treated controls (Fig. 4F and F`), as were the expression levels of *Ptch1* and *Gli1* (Fig. 4C, C`, D, D`, G, G`, H, H`). In particular, *Ptch1* was strongly expressed in palatal ridge epithelium as well as the underlying mesenchyme in the PBS-treated controls (Fig. 4C`). After 5E1 treatment, mesenchymal expression of *Ptch1* was markedly reduced (Fig, 4G`). *Bmp4* expression was not detected at E13.5 in either the PBS- or 5E1-treated animals (Fig. 4I, I`, L, L`). In the PBS-injected group, *Lef1* was expressed in the epithelium of the rugae region (Fig. 4J and J`). However, the expression of *Lef1* was expanded in the 5E1-treated group (Fig. 4M and M`). *Lrp4* was not expressed in the palatal ridges in either PBS- and 5E1-treated animals (Fig. 4K, K`, N, N`).

Gene expression was examined further after palatal fusion (Fig. 5). At E14.5, strong *Shh* expression remained along the nine palatal ridge lines in the PBS-treated controls (Fig. 5A and A`). In contrast, the pattern of *Shh* expression was disturbed by 5E1 injection (Fig. 5E and E`). *Sostdc1* was expressed in the palatal epithelium, except along the rugae region in the

PBS-treated controls (Fig. 5B and B`). After 5E1 injection, *Sostdc1* expression was dramatically reduced in the palatal epithelium (Fig. 5F and F`). *Ptch1* was strongly expressed in the palatal epithelium and beneath mesenchyme in the controls (Fig. 5C and C`) but was markedly reduced after 5E1 injection (Fig. 5G and G`). The *Gli1* expression was lower after 5E1 treatment compared to the PBS controls (Fig. 5D, D`, H, H`). *Bmp4* was strongly expressed in the anterior region of the rugae palatine (Fig. 5I). Sectioning revealed that *Bmp4* was expressed in the underlying mesenchyme of the anterior three rugae (Fig. 5I`). However, mesenchymal *Bmp4* expression was observed in the first anterior rugae after 5E1 treatment (Fig. 5L and L`). *Lef1* was expressed weakly along the epithelium of the nine rugae lines in the PBS-treated group (Fig. 4J and J`). After 5E1 injection, *Lef1* was not expressed along the rugae line, although a substantial area of the ”dotted” expression pattern of *Lef1* was detected in the palatal epithelium (Fig. 5M and M`). 5E1 treatment did not affect the *Lrp4* expression pattern (Fig. 5K, K`, N, N`).

The gene expression levels were further investigated using microarrays and real-time quantitative polymerase chain reaction (RT-qPCR). 5E1treatment increased *Shh* expression,,left the levels of *Bmp4*, *Lrp4* and *Lef1* expression unchanged (Fig. 6A and B), and reduced the expression levels of *Sostdc1*, *Ptch1* and *Gli1*. (Fig. 6A and B).

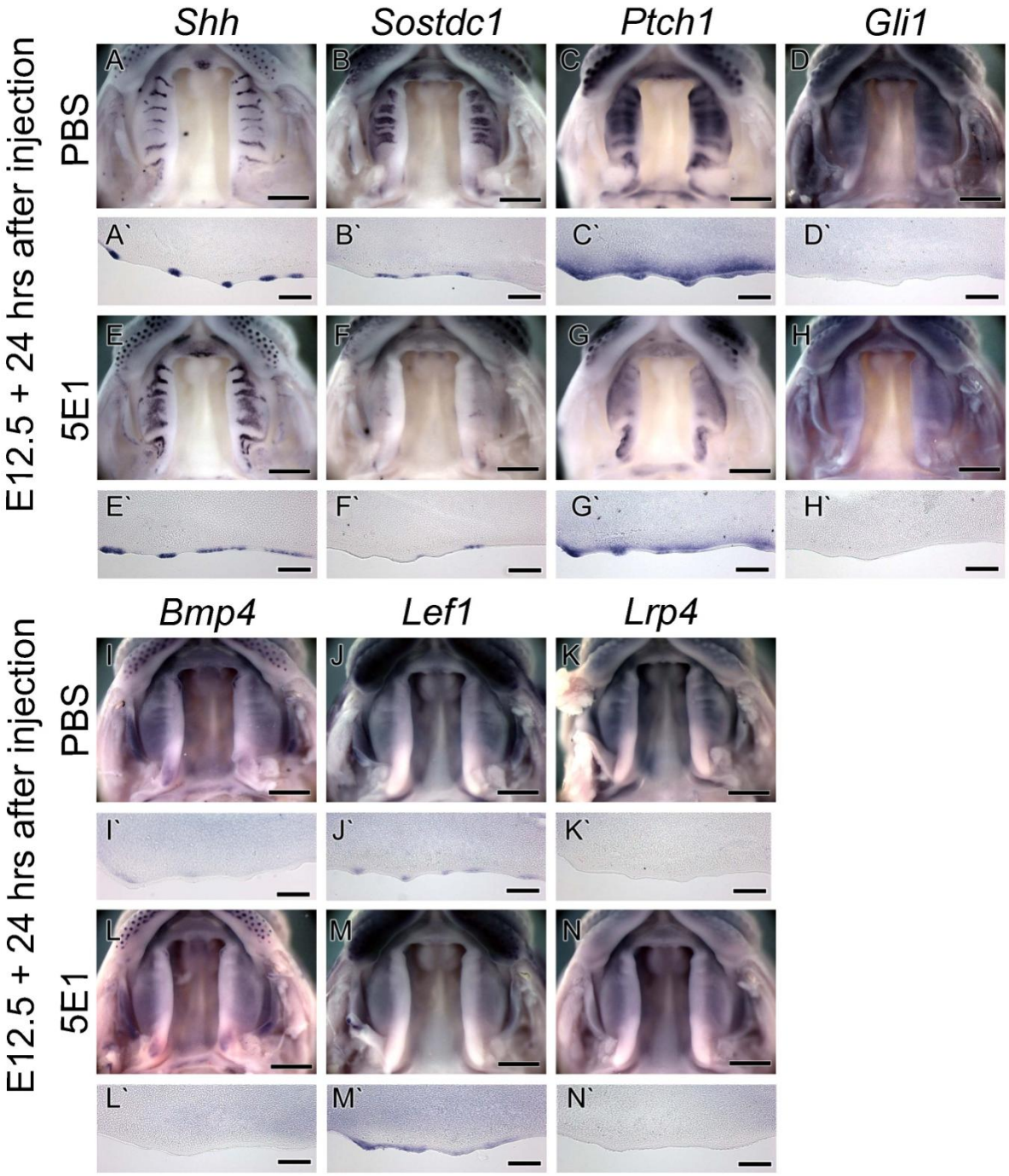
Shh
Sostdc1
Ptch1
Gli1
E12.5 + 24 hrs after injection
PBS
5E1
A
B
C
D
A`
B`
C`
D`
E
F
G
H
E`
F`
G`
H`
Bmp4
Lef1
Lrp4
E12.5 + 24 hrs after injection
PBS
5E1
I
J
K
I`
J`
K`
L
M
N
L`
M`
N`

Fig.4. Alteration of gene expression pattern in rugae 24 hours after 5E1 injection. (A, A`, E, E`) *Shh* expression pattern is altered 24 hours after 5E1 treatment. Expanded *Shh* expression is detected in 5E1 treated palatal shelves. (B, B`, C, C` F, F`, G, G`) *Sostdc1* and *Ptc1* expression are remarkably reduced in palatal ridge 24 hours after 5E1 delivery. (D, D`, H, H`, I, I`, L, L`, K, K`) *Gli1*, *Bmp4* and *Lrp4* expression are not altered after 5E1 injection. (J, J`, M, M`) Lef1 expression pattern is changed after 5E1 treatment. *Lef1* is expressed rugae and inter rugae region after 5E1 injection. Scale bar; A-N : 500 μm, A`-N` : 100 μm.

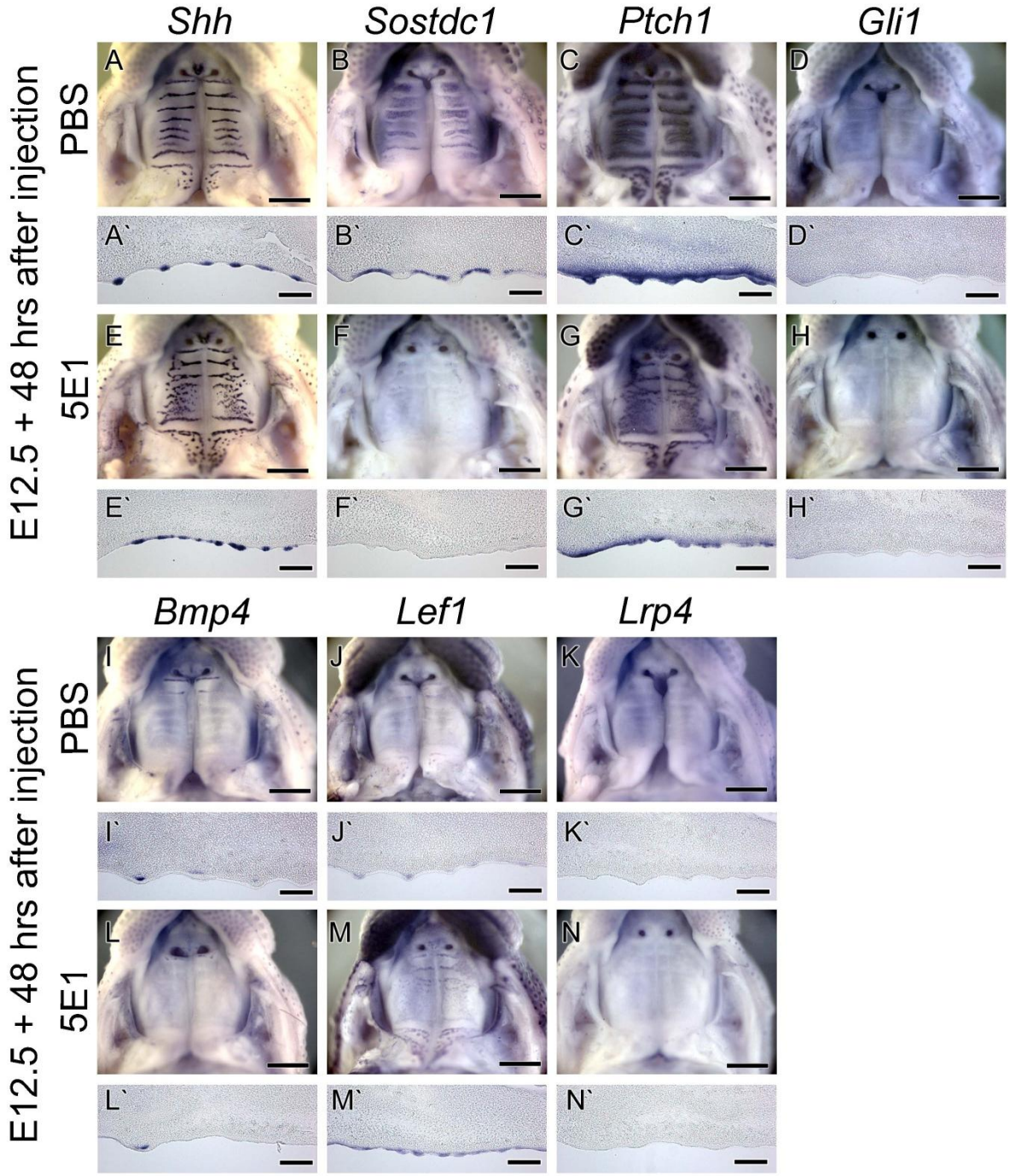
Shh
Sostdc1
Ptch1
Gli1
E12.5 + 48 hrs after injection
PBS
5E1
A
B
C
D
A`
B`
C`
D`
E
F
G
H
E`
F`
G`
H`
Bmp4
Lef1
Lrp4
I
J
K
I`
J`
K`
L
M
N
L`
M`
N`

Fig.5. Alteration of gene expression pattern in rugae 48 hours after 5E1 injection. (A, A`, E, E`) Line shaped *Shh* expression pattern is altered after 5E1 treatment. Dotted and expanded *Shh* expression is detected in fused palate 48 hours after 5E1 treated. (B, B`, C, C` F, F`, G, G`) *Sostdc1* and *Ptc1* expression are clearly reduced in palatal ridge 48hours after 5E1 delivery. (D, D`, H, H`, K, K`) Gli1 and *Lrp4* expression are not altered after 5E1 injection. (I, I`, L, L`) In control group, *Bmp4* was expressed in the underlying mesenchyme of the anterior three rugae. However, mesenchymal *Bmp4* expression was observed in the first anterior rugae after 5E1 treatment. (J, J`, M, M`) In control group which is injected the PBS, *Lef1* is expressed in epithelium of palatal ridge. However, *Lef1* is expressed in the rugae and inter-rugae region in 5E1 injected group. Scale bar; A-N : 500 μm, A`-N` : 100 μm.

A

Gene Symbol	Gene Title	Reference Sequence	Fold Change 5E1 vs PBS
Up-regulated gene			
Shh	sonic hedgehog	NM_009170	2.09186
Not changed genes			
Bmp4	bone morphogenetic protein 4	NM_007554	1.23090
Lrp4	low density lipoprotein receptor-related protein 4	NM_172668	1.16853
Lef1	lymphoid enhancer binding factor 1	NM_010703	-1.07990
Down-regulated genes			
Sostdc1	sclerostin domain containing 1	NM_025312	-1.63200
Ptch1	patched homolog 1	NM_008957	-2.17603
Gli1	GLI-Kruppel family member GLI1	NM_010296	-2.45339

B

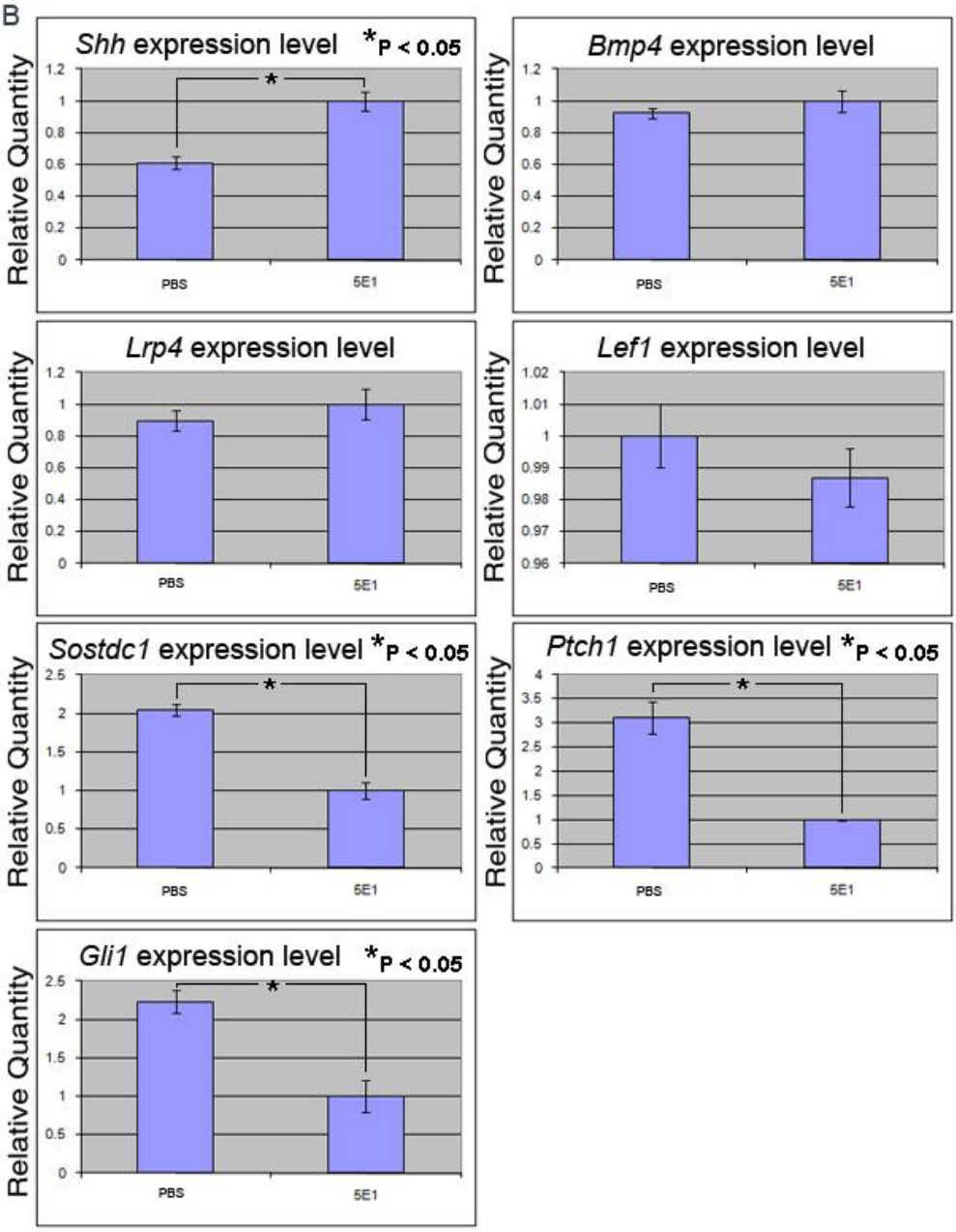

Fig.6. Alteration of gene expression level after 5E1 injection. (A) Gene expression level is examined by microarray. (B) Gene expression level was determined using real-time qPCR. *Shh* expression level is up-regulated after 5E1 treatment. *Bmp4*, *Lef1* and *Lrp4* expression level are not changed by 5E1 injection. Expression level of *Sostdc1*, *Ptch1* and *Gli1* are down-regulated by 5E1.

3. Cell proliferation and apoptosis are regulated by *Shh* signaling during rugae formation.

To further elucidate the relationship between *Shh* signaling and rugae formation, Ki67 and terminal deoxynucleotidyl transferase dUTP nick end labeling (TUNEL) staining was examined after 5E1 injection at E12. The PBS-treated control group showed increased epithelial thickness (the placode) along the rugae at E13.5 (Fig. 7A and D). However, placode formation was not observed 24hours after 5E1 injection (Fig. 7G and J). Ki67-positive proliferating cells were observed in the palatal epithelium and mesenchyme at 24 hours after PBS injection. However, Ki67-positive cells were not clearly detected in the placode regions that form the rugae palatine in the PBS-treated control group (Fig. 7B and E). After 5E1 injection, Ki67-positive cells were localized throughout the palatal epithelium as well as in the mesenchyme (Fig. 7H and K). TUNEL-positive apoptotic cells were detected in the tip of the placodes after PBS treatment (Fig. 7C and F). No apoptotic cells were observed in either the epithelium or the mesenchyme at 24 hours after 5E1 treatment (Fig. 7I and L).

The number of regions showing increased epithelial thickness in the developing palate was greater at 48 hours after 5E1 injection than in the PBS-treated group (Fig. 8A, D, G, J). The distribution of Ki67-positive cells at 48 hours post-PBS injection was similar to that observed at 24 hours postinjection: Ki67-positive cells were not localized in the rugae region (Fig. 8B and E).At 48 hours after 5E1 injection, localization of Ki67 positive cells was altered compared to the control condition. In some regions of the epithelium, Ki67-positive cells were not observed even though epithelial thickening did not occur (Fig. 8H and K). A few TUNEL-positive cells were observed in the tip of the palatine ridges at 48 hours after PBS treatment (Fig. 8C and F). However, the number of TUNEL-positive cells was increased in both the epithelium and mesenchyme, including in the non-thickened palatal epithelium, at 48 hours after 5E1 injection (Fig. 8I and L).

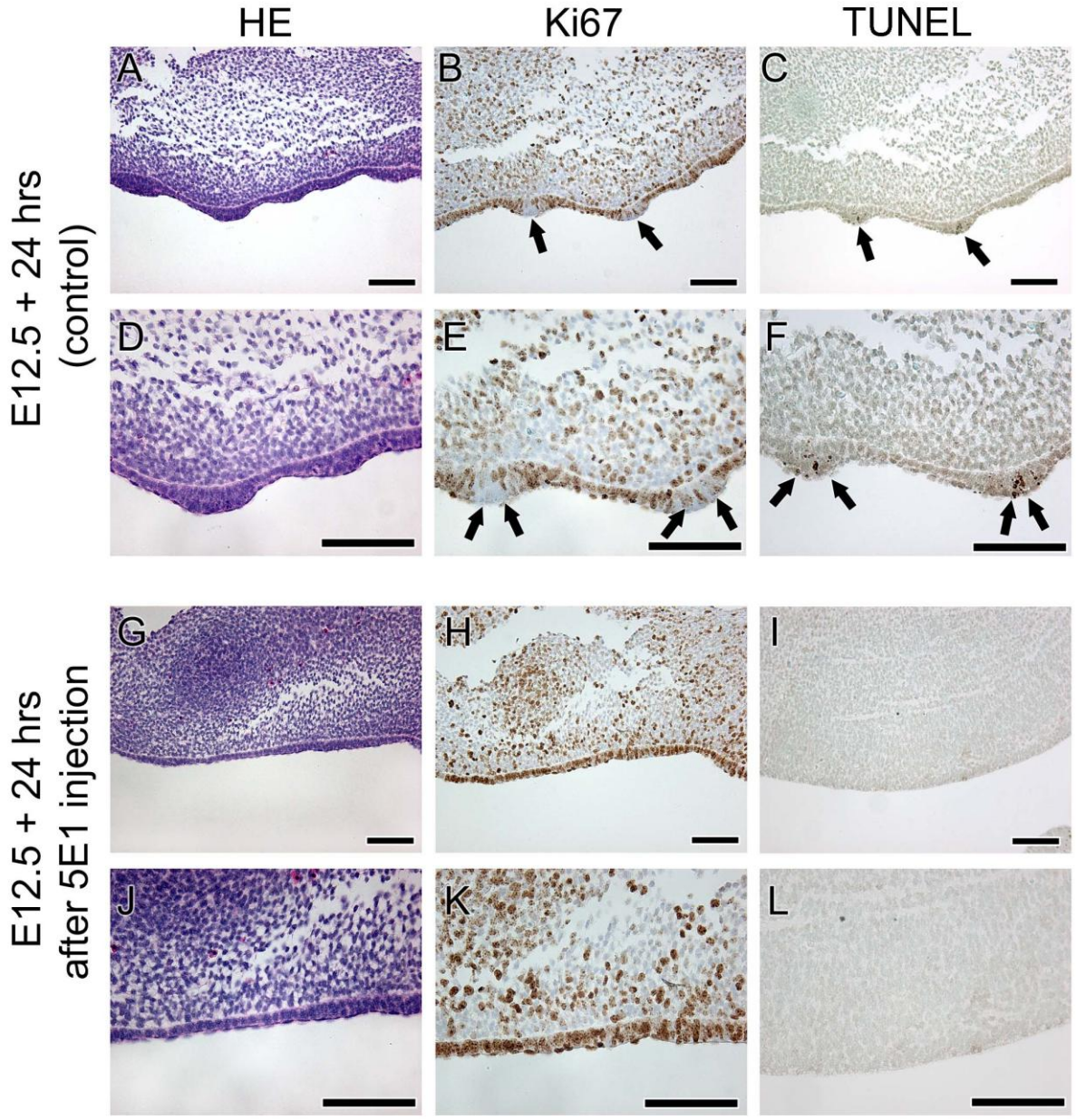
HE
Ki67
TUNEL
E12.5 + 24 hrs
(control)
E12.5 + 24 hrs
after 5E1 injection
A
B
C
D
E
F
G
H
I
J
K
L

Fig.7. Alteration of molecular events 24 hours after 5E1 treatment. (A, D) Epithelial thicknesses are observed in PBS treated control group at E13.5. (G, J) After 5E1 injection, epithelial thickness is not detected at E13.5. (B, E) Ki67 positive proliferating cells are localized both in palatal epithelium and mesenchyme except tip of rugae epithelium at E13.5. (H, K) Ki67 positive cells are observed both in palatal epithelium and mesenchyme after 5E1 injection. (C, F) TUNEL positive apoptotic cells are localized at the tip of the palatal rugae epithelium at E13.5. (I, L) TUNEL positive cells are not detected in developing palate after 5E1 treatment. Scale bar; A-L : 100 μm.

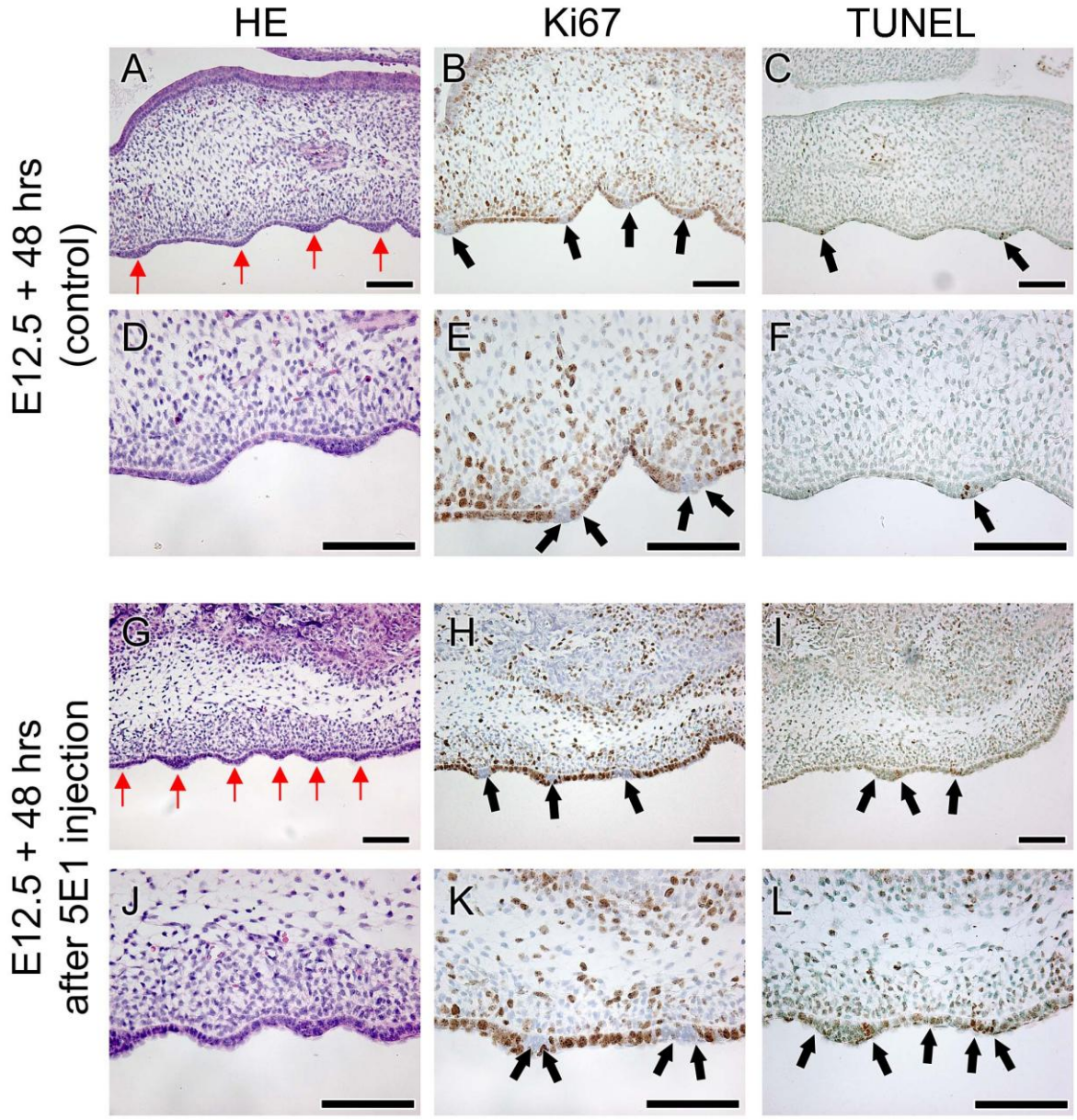
HE
Ki67
TUNEL
E12.5 + 48 hrs (control)
E12.5 + 48 hrs after 5E1 injection
A
B
C
D
E
F
G
H
I
J
K
L

Fig.8. Alteration of molecular events 48 hours after 5E1 treatment. (A, D) Epithelial placodes are observed in PBS treated control group at E14.5. (G, J) After 5E1 injection, more epithelial thicknesses are observed at E14.5 compared to PBS control group. (B, E) Ki67 positive proliferating cells are localized in palatal epithelium except tip of rugae epithelium at E14.5. (H, K) Ki67 positive cells are not detected in the epithelial thickness not formed region after 5E1 injection. (C, F) TUNEL positive apoptotic cells are localized at the tip of the palatal ridge epithelium at E14.5. (I, L) TUNEL positive cells are observed both in epithelium and mesenchyme after 5E1 treatment. Scale bar; A-L : 100 μm.

4. *Sostdc1* is regulated by *Shh* signaling during rugae development.

To confirm the relationship between *Shh* signaling and *Sostdc1*, gene expression was examined after a SHH-protein-soaked bead was implanted into a palate from which the epithelium had been removed at E12.5. At 24 hours after PBS-soaked bead implantation, *Sostdc1* and *Ptch1* expression were not expressed around the bead (Fig. 9A and C). However, *Sostdc1* and *Ptch1* were strongly induced around the SHH-protein-soaked bead (Fig. 9B and D). After sectioning, it was also evident that PBS did not induce *Sostdc1* and *Ptch1* expression in epithelium-free palatal mesenchyme (Fig. 9A` and C`). It was substantiated by sectioning that *Sostdc1* expression was rescued around the SHH soaked bead in epithelial removed palatal mesenchyme (Fig. 9B`). SHH also strongly induced *Ptch1* expression in the palatal mesenchyme (Fig. 9D`).

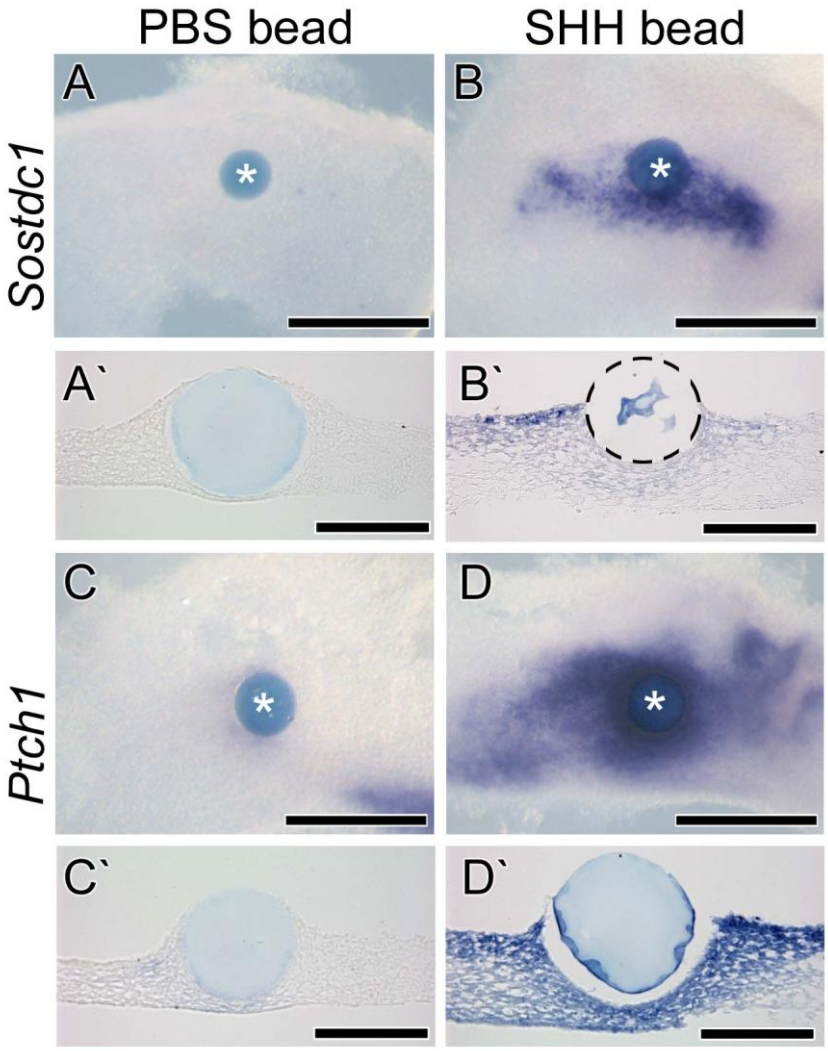

Fig.9. *Sostdc1* and *Pcth1* expression pattern after SHH bead implantation. (A, A`, C, C`) *Sostdc1* and *Pcth1* was not rescued around PBS-soaked beads in the epithelium removed palatal mesenchyme. (B, B`, D, D`) SHH-soaked beads are strongly induced *Sostdc1* and *Pcth1* in epithelium removed palatal mesenchyme. Asterisks and black dotted circle : bead, Scale bar; A, B, C, D: 500 μm, A`, B`, C`, D`: 100 μm.

5. Palatal ridges follow the reaction-diffusion model for correct pattern formation.

During palatal rugae formation, *Lef1* was expressed in the rugae placode (Fig. 4J and J`), while *Sostdc1* expression was detected in inter-rugae region, which was outside of *Lef1* expression region (Fig. 4B and B`). Previous studies have found that *Wnt* signaling induces the expression of *Lef1* and *Shh* in other organs during development such as tooth (Kratochwil *et al*., 2002; Liu *et al*., 2008). Moreover, *Wnt* signaling is regulated by *Sostdc1* (Ahn *et al*., 2010). Based of these results, we used the reaction-diffusion model to analyze our data in an ttempt to explain the rugae patterning. The model included *Wnt*, *Shh* and *Sostdc1* as the activator, mediator and inhibitor, respectively (Fig. 10B). Analyses of the interactions between *Wnt*, *Shh* and *Sostdc1*,which were conducted using mathematical simulation (Fig. 10C), revealed the following.

1. Activator signaling was higher in rugae area than inter-rugae region.
2. Mediator signaling occurred in the same medial region as the activator, but its range was wider than that of the activator
3. Inhibitor signaling was higher in inter-rugae regions in order to avoid ectopic activator expression in these regions (Fig. 10C).

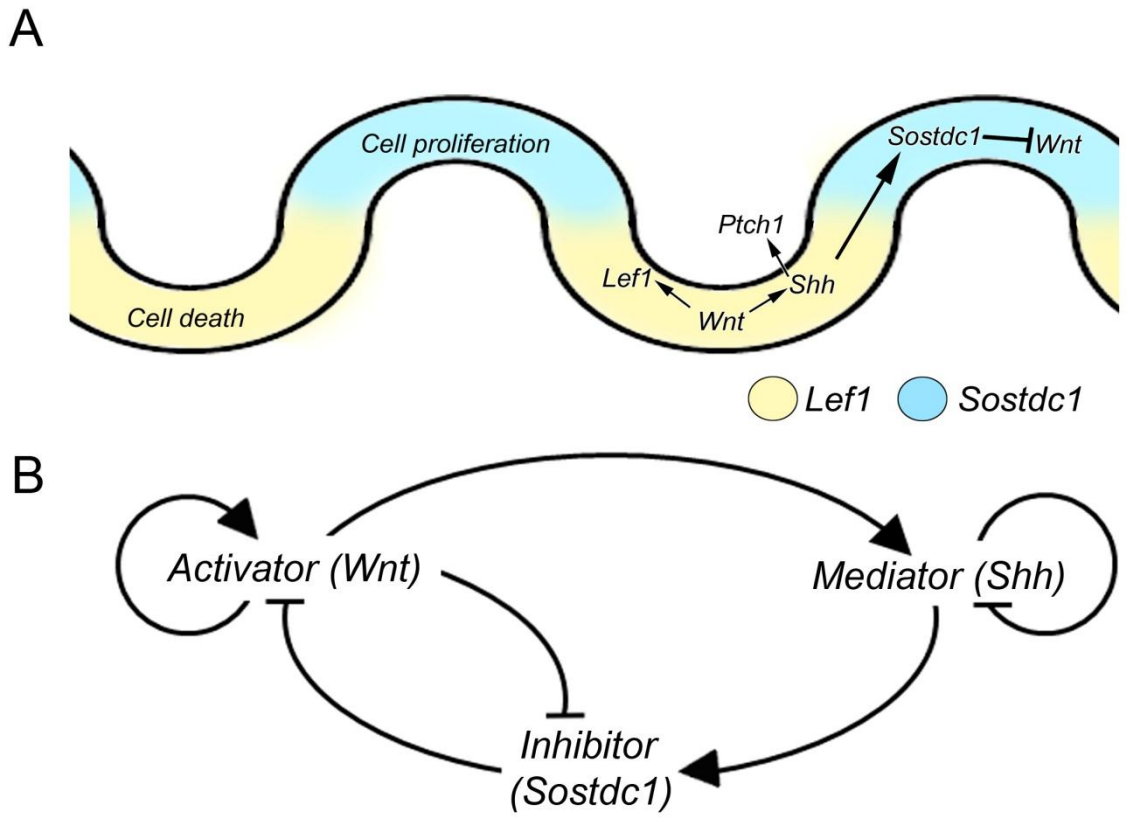
A
Cell proliferation
Cell death
Sostdc1
Wnt
Ptch1
Lef1
Shh
Wnt
Lef1
Sostdc1
B
Activator (Wnt)
Mediator (Shh)
Inhibitor
(Sostdc1)
C
Activator
(Wnt)
Mediator
(Shh)
Inhibitor
(Sostdc1)
1
2
3
4
5
6
7
8
9
5
4.5
4
3.5
3
2.5
2
1.5
1
0.5
0

Fig.10. Schematic diagram of developing palatal rugae. (A) Schematic of relationship among the *Wnt*, *Shh* and *Sostdc1* in developing palatal rugae. Wnt signals in rugae induce *Shh* expression. Secreted *Shh* in rugae moves laterally to induce *Sostdc1*. *Sostdc1*-expressing area (*Sostdc1* area) complements the *Lef1*-expressing area (*Lef1* area). (B) Schematic diagram of the reaction–diffusion model showing interactions among activator (*Wnt*), mediator (*Shh*) and inhibitor (*Sostdc1*). (C) Mathematical simulation of activator, mediator and inhibitor pattern show 9 palatal rugae in PBS treated control group mice.

IV. Discussion

1. Rugae patterns are disturbed by inhibition of *Shh* signaling.

Nine palatal ridges are formed during mouse secondary palate development (Sakamoto *et al*., 1989).). The first ruga starts to form between E12 and E13, with thickening of the epithelium. The number of rugae increases conspicuously between E13 and E14 (Peterková *et al*., 1987). In the present study, scanning electron microscopy revealed mountain-range-like rugae at E12.5 (Fig. 3A and D). In controls injected with PBS, nine rugae lines were detected in the fused palate at 96 hours postinjection (Fig. 3B and E). The relationship between *Shh* signaling and rugae formation was investigated by injecting 5E1, an IgG1 monoclonal antibody against Shh protein, into pregnant mice to block *Shh* signaling (Wang *et al*., 2000). After blocking the *Shh* signaling, rugae lost their linear shape and developed into a scattered pattern of dot-shaped rugae (Fig. 3C and F). These findings indicate that *Shh* signaling plays a pivotal role in the formation of the correct rugae pattern.

2. Wnt and *Sostdc1* are target of *Shh* signaling during spatial patterning of palatal rugae.

Shh is expressed in the thickened palatal ridge epithelium, which forms the rugae palatinae on the secondary palate (Bitgood and McMahon, 1995). Moreover, *Shh* signaling has been demonstrated to play essential roles in craniofacial development (Chiang *et al*., 1996). Several studies have found that Wnt family members play important roles during orofacial morphogenesis (Brown *et al*., 2003; Blanton *et al*., 2004; Juriloff *et al*., 2006; Lan *et al*., 2006; Lee *et al*., 2008). In particular, LEF1 is expressed in most embryonic tissues and plays a crucial role in palatogenesis (Mohamed *et al*., 2004; Nawshad and Hay, 2003). The

present study found that *Shh* was strongly expressed along the epithelium of the nine palatine ridges at both E13.5 and E14.5 (Fig. 4A, A`; 5A, A`), while *Sostdc1* was intensely expressed in the epithelium of the inter-rugae regions (Fig. 4B, B`; 5B, B`). However, after blocking of the Shh signaling by 5E1, the expression of *Shh* expanding into the inter-rugae regions (Fig. 4E, E`; 5E, E`) with a concurrent reduction of *Sostdc1* expression in inter-rugae regions (Fig. 4F, F`; 5F, F`). Implanting SHH-soaked beads induced *Sostdc1* expression around the bead (Fig. 9B) , confirming a direct relationship between *shh* and *Sostdc1* expression. *Lef1* was weakly expressed in the tip of palatal ridge epithelium (Fig. 4J, J`; 5J, J`). After 5E1 treatment, *Lef1* was not restricted to the area along the rugae line, but formed a dotted pattern of expression throughout the secondary palate (Fig. 4M, M`; 5M, M`). Our results indicate that *Sostdc1* can be induced by shh in developing palatal ridge for correct rugae formation. Moreover, loss of *Sostdc1* by blocking the *Shh* signaling induced ectopic *Wnt* signaling during palatal ridge development.

3. Downstream genes of *Wnt* and *Shh* signaling are altered by 5E1.

The Hh signaling receptor *Ptch1* and transcriptional activator *Gli1* are regulated by *Shh* signaling (Chen and Struhl, 1996; Goodrich *et al*., 1996, 1997). We examined the expression pattern of both *Ptch1* and *Gli1* after 5E1 injection. *Ptch1* expression was reduced in the epithelium as well as the mesenchyme around the rugae region (Fig. 4C, C`, G, G`; 5C, C`, G, G`). *Gli1* expression also reduced in developing palate (Fig. 4D, D`, H, H`; 5D, D`, H, H`). These results confirm that *Shh* signaling is required to regulate the expressions of *Ptch1* and *Gli1* in developing palate.

Epithelial *Shh* signaling is closely related to both the mesenchymal *Fgf* and *Bmp* pathways regulating cell proliferation during palatogenesis (Rice *et al*., 2004; Zhang *et al*., 2002). We have observed that *Bmp4* was expressed in palatal mesenchyme just beneath the

rugae epithelium along the first three rugae line at E14.5 (Fig. 5I and I`), whereas only the first palatal ruga was *Bmp4* positive after blocking of the *Shh* signaling by 5E1 (Fig. 5L and L`). These results suggest that correct rugae formation is dependent on Shh signaling being closely related to Bmp signaling.

Both the gene expression pattern and gene expression level of *Shh* were affected by 5E1 (Fig. 6). *Shh* expression was induced, whereas *Sostdc1*, *Ptch1*, and *Gli1* expression levels were reduced after 5E1 treatment, indicating that *Shh* signaling plays an important role in preserving the correct gene expression levels during rugae differentiation. Scanning electron microscopy results indicate that the shape of the palatal ridges changed from a ridge shape to a dotted conformation corresponding to *Shh* and *Lef1* expression patterns. Thus, palatal ridge development may be governed directly by *Shh* signaling.

4. Cell proliferation and apoptosis are regulated by *Shh* signaling during rugae development.

Epithelial expression of *Shh* is closely related to both the mesenchymal *Fgf* and *Bmp* pathways. *Fgf* and *Bmp* signaling are regulators of a cascade that regulates cellular events such as proliferation during palatogenesis (Rice *et al*., 2004; Zhang *et al*., 2002). At 24 hours after PBS injection, areas of thickening were detected in the palatal epithelium (Fig. 7A). Ki67-proliferating cells were not observed in these placodes, but TUNEL-positive apoptotic cells were detected (Fig. 7E and F). In contrast, 24 hours after 5E1 treatment, no placodes were observed in the palatal epithelium (Fig. 7G), along with proliferating cells throughout the palatal epithelium (Fig. 7H). Apoptotic cells were not observed in the developing palate (Fig. 7I). However, more placodes were observed in the palatal epithelium at 48 hours after 5E1 injection compared to 48 hours after PBS injection in the control group (Fig. 8A and G). In the former, some areas without epithelial thickening were found where proliferating cells

were absent (Fig. 8K). Moreover, apoptotic cells were dramatically up-regulated in both the palatal epithelium and the mesenchyme at 48 hours after 5E1 treatment (Fig. 8L). These results provide evidence that the mechanism underlying *Shh* signaling to ensure correct rugae formation during their development involves the regulation of cell proliferation and apoptosis.

5. Wnt, Shh and *Sostdc1* interactions govern the correct patterning of palatal ridges.

Wnt signaling acts like an activator of rugae patterning. A previous study found ectopic expression of *Shh* expression in the molars and rugae of *Lrp4*$^{-/-}$ mice (Ohazama *et al*., 2008). We have demonstrated that an SHH-soaked bead induced *Sostdc1* expression in epithelium-free palatal mesenchyme (Fig. 9B and B`), substantiating the idea that *Sostdc1* is regulated by mediator *Shh* signaling. We postulate that the palatal ridges have both a *Lef1*-expression activation zone and a Sostdc1-expression inhibition zone within the *Wnt*, *Shh*, and *Sostdc1* loop, which in effect acts to separate the nine palatal ridges from each other (Fig. 10A). After blocking of SHH protein by 5E1, the pattern of *Lef1* expression was disrupted, from a striped to a dotted conformation, as was seen for the *Shh* expression pattern (Fig. 5M and M`). Moreover, *Sostdc1* expression was not found in developing palatal ridges after 5E1 treatment (Fig. 5F and F`). The *Lef1*-expression activation zone was altered to an irregular dotted pattern and the *Sostdc1*-expression inhibition zone disappeared after 5E1 treatment. Thus, down-regulated *Shh* signaling could not induce the appropriate *Sostdc1* expression. The normal striped shape of the rugae was therefore not retained, as a consequence of the altered *Wnt* signaling caused by the loss of *Sostdc1*, leaving an abnormal dotted rugae shape in a nonspecific palate region (Fig. 10B). Based on this idea, we applied a mathematical simulation to the normal palatal ridge patterning and 5E1-treated irregular patterning. The PBS-treated control group followed the reaction-diffusion model for creating a striped pattern

of palatal ridges (Fig. 10C). However, the 5E1-treated group deviated from the reaction-diffusion model because of the absence of inhibitor, *Sostdc1*. Loss of *Sostdc1* induced an irregular dotted rugae conformation, which is attributable to a failure to inhibit the activator (*Wnt* signaling). Mathematical simulation therefore makes it possible to verify the spatial allocation of the important factors in the previously published reaction–diffusion model. These interactions may be essential for correct palatal ridge pattern formation in wild-type mice.

V. Conclusion

We have demonstrated by *in situ* hybridization, microarray, and RT-qPCR assays that *Shh* regulates several genes during palatal ridge formation. Due to the strong correlation of *Shh* with *Sostdc1*, *Ptch1* and *Lef1* expression, our findings suggest a mechanism for correct palatal ridge development following the reaction–diffusion model, thereby clarifying the relationships between *Wnt*, *Shh*, and *Sostdc1*. Mathematical simulation was used to establish that crosstalk between *Wnt*, *Shh*, and *Sostdc1* governs the correct patterning of palatal ridges, suggesting that these relationships play crucial roles during the correct spatial patterning of other organs that express *Wnt*, *Shh*, and *Sostdc1*.

VI. References

1. Gritli-Linde A (2007) Molecular control of secondary palate development. *Dev Biol* 301:309-326.

2. Ferguson MW (1987) Palate development: mechanisms and malformations. *Ir J Med Sci* 156:309-315.

3. Eisentraut M (1979) Das Gaumenfaltenmuster der Säugetiere und seine Bedeutung für Stammesgeschichtliche und taxonomische Untersuchungen. *Bonner Zool Monogr* 8:211-214.

4. Pantalacci S, *et al*. (2008) Patterning of palatal rugae through sequential addition reveals an anterior/posterior boundary in palatal development. *BMC Dev Biol* 8:116-133.

5. Sakamoto MK, Nakamura K, Handa J, Kihara T, Tanimura T (1989) Morphogenesis of the secondary palate in mouse embryos with special reference to the development of rugae. *Anat Rec* 223:299-310.

6. Mitsui C, Iwanaga T, Yoshida S, Kawasaki T (2000) Immunohistochemical demonstration of nerve terminals in the whole hard palate of rats by use of an antiserum against protein gene product 9.5 (PGP 9.5). *Arch Histol Cytol* 63:401-410.

7. Ichikawa H, Matsuo S, Silos-Santiago I, Jacquin MF, Sugimoto T (2001) Developmental dependency of Merkel endings on trks in the palate. *Brain Res Mol Brain Res* 88:171-175.

8. Kido MA, Muroya H, Yamaza T, Terada Y, Tanaka T (2003) Vanilloid receptor expression in the rat tongue and palate. *J Dent Res* 82:393-397.

9. Nunzi MG, Pisarek A, Mugnaini E (2004) Merkel cells, corpuscular nerve endings and free nerve endings in the mouse palatine mucosa express three subtypes of vesicular glutamate transporters. *J Neurocytol* 33:359-376.

10. Porntaveetus T, Oommen S, Sharpe PT, Ohazama A (2010) Expression of Fgf signalling pathway related genes during palatal rugae development in the mouse. *Gene Expr Patterns* 10:193-198.

11. Rice R, *et al*. (2004) Disruption of Fgf10/Fgfr2b-coordinated epithelial-mesenchymal interactions causes cleft palate. *J Clin Invest* 113:1692-1700.

12. Tyler MS, Koch WE (1977) In vitro development of palatal tissues from embryonic mice. II. Tissue isolation and recombination studies. *J Embryol Exp Morphol* 38:19-36.

13. Zhang Z, *et al*. (2002) Rescue of cleft palate in Msx1-deficient mice by transgenic Bmp4 reveals a network of BMP and Shh signaling in the regulation of mammalian palatogenesis. *Development* 129:4135-4146.

14. Bitgood MJ, McMahon AP (1995) Hedgehog and Bmp genes are coexpressed at many diverse sites of cell-cell interaction in the mouse embryo. *Dev Biol* 172:126-138.

15. Chiang C, Litingtung Y, Lee E, Young KE, Corden JL, Wesphal H, Beachy P (1996)

Cyclopia and defective axial patterning in mice lacking Sonic hedgehog gene function. *Nature* 383:407-413.

16. Chen Y, Struhl G (1996) Dual roles for patched in sequestering and transducing Hedgehog. *Cell* 87:553-563.

17. Goodrich LV, Johnson RL, Milenkovic L, McMahon JA, Scott MP (1996) Conservation of the hedgehog/patched signaling pathway from flies to mice: induction of a mouse patched gene by Hedgehog. *Genes Dev* 10:301-312.

18. Goodrich LV, Milenkovic L, Higgins KM, Scott MP (1997) Altered neural cell fates and medulloblastoma in mouse patched mutants. *Science* 277:1109-1113.

19. Brown NL, *et al*. (2003) Microarray analysis of murine palatogenesis: temporal expression of genes during normal palate development. *Dev Growth Differ* 45:153-165.

20. Blanton SH, *et al*. (2004) Association of chromosomal regions 3p21.2, 10p13, and 16p13.3 with nonsyndromic cleft lip and palate. *Am J Med Genet A* 125:23-27.

21. Juriloff DM, Harris MJ, McMahon AP, Carroll TJ, Lidral AC (2006) Wnt9b is the mutated gene involved in multifactorial nonsyndromic cleft lip with or without cleft palate in A/WySn mice, as confirmed by a genetic complementation test. *Birth Defects Res A Clin Mol Teratol* 76:574-579.

22. Lan Y, *et al*. (2006) Expression of Wnt9b and activation of canonical Wnt signaling

during midfacial morphogenesis in mice. *Dev Dyn* 235:1448-1454.

23. Lee JM, *et al*. (2008) Wnt11/Fgfr1b cross-talk modulates the fate of cells in palate development. *Dev Biol* 314:341-350.

24. Mohamed OA, Clarke HJ, Dufort D (2004) Beta-catenin signaling marks the prospective site of primitive streak formation in the mouse embryo. *Dev Dyn* 231:416-424.

25. Nawshad A, Hay ED (2003) TGF[beta]3 signaling activates transcription of the LEF1 gene to induce epithelial-mesenchymal transformation during mouse palate development. *J Cell Biol* 163:1291-1301.

26. Johnson EB, Hammer RE, Herz J (2005) Abnormal development of the apical ectodermal ridge and polysyndactyly in Megf7-deficient mice. *Hum Mol Genet* 14:3523-3538.

27. Wang LC, *et al*. (2000) Regular articles: conditional disruption of hedgehog signaling pathway defines its critical role in hair development and regeneration. *J Invest Dermatol* 114:901-908.

28. Kratochwil K, Galceran J, Tontsch S, Roth W, Grosschedl R (2002) FGF4, a direct target of LEF1 and Wnt signaling, can rescue the arrest of tooth organogenesis in Lef1$^{-/-}$ mice. *Genes Dev* 16:3173-3185.

29. Liu F, *et al*. (2008) Wnt/beta-catenin signaling directs multiple stages of tooth morphogenesis. *Dev Biol* 313:210-224.

30. Ahn Y, Sanderson BW, Klein OD, Krumlauf R (2010) Inhibition of Wnt signaling by Wise (Sostdc1) and negative feedback from Shh controls tooth number and patterning. *Development* 137:3221-3231.

31. Peterková R, Klepácek I, Peterka M (1987) Prenatal development of rugae palatinae in mice: scanning electron microscopic and histologic studies. *J Craniofac Genet Dev Biol* 7:169-189.

32. Ohazama A, *et al*. (2008) Lrp4 modulates extracellular integration of cell signaling pathways in development. *PLoS One* 3:e4092.

ABSTRACT (in Korean)

입천장주름 발생에 있어 *Shh*의 역할

<지도교수 최병재>

연세대학교 대학원 치의학과

강 대 운

포유동물의 2차 구개발생은 복잡한 분자생물학적, 세포학적 활동이 동반되는 매우 중요한 과정이다. 물결모양의 입천장 주름은 대부분의 포유류의 경구개 부위에서 볼 수 있다. 하지만 그 수와 배열은 종에 따라 차이가 있으며 생쥐의 2차 구개에서는 9개의 입천장주름을 발견할 수 있다. 상피와 간엽의 상호작용을 통한 신호전달은 2차 구개의 발생에 매우 중요한 역할을 한다고 알려져 있으며 상피에서의 *Shh*신호는 간엽의 *Fgf*, *Bmp*와 매우 밀접한 관계를 지니고 있다고 알려져 있다. 생쥐는 세포막 수용체인 *Ptch1* 혹은 *Ptch2* 와 결합할 수 있는 Hh ligand를 분비하며 *Gli1*과 *Gli2*는 Hh signaling의 전사 활성인자로 알려져 있다. 또한 *Lef1* 을 포함하는 *Wn*t family는 구강악안면형성과정에 있어 중요한 역할을 한다. 본 연구에서는 *Shh*을 억제하는 항체인 5E1(anti-SHH antibody)을 어미 태반을 통해 배아에 투여하여 SHH 단백질의 활성을 일시적으로 차단하였다. 그 결과 대조군에서는 산맥(ridge)형태의 입천장 주름이 관찰되었으나 실험군에서는 산(dot)모양으로 변하였다. 이러한 입천장주름의 모양이 변화하는 동안 상호작용

하는 유전자들을 알아보기 위해 E12.5일에 5E1을 처리한 후 microarray와 RT-qPCR 방법을 이용하여 유전자 발현량의 변화를 분석하였다. 그 결과 *Shh*의 발현량이 증가하였고 반대로 *Sostdc1, Ptch1, Gli1*은 감소함을 알 수 있었다. 또한 SHH protein bead와 수학적 분석법(mathematical simulation)을 이용하여 여러 유전자들 간의 상관관계를 확인하였다. 이상의 실험을 통해 *Sostdc1*은 *Wnt* pathway의 길항제이며 *Shh*의 downstream target임을 알게 되었고 *Wnt, Shh, Sostdc1* 간의 상호 작용은 입천장 주름의 정상적인 공간적 패턴을 결정하는데 있어 매우 중요한 역할을 함을 알 수 있었다.

핵심되는 말 : 입천장 주름 형성, 5E1, *Shh, Wnt, Sostdc1*